The EMBO Journal Vol.17 No.17 pp.5001–5014, 1998

The alternative product from the human *CDKN2A* locus, p14^{ARF}, participates in a regulatory feedback loop with p53 and MDM2

Francesca J.Stott[1], Stewart Bates[2], Marion C.James[1], Beth B.McConnell[1], Maria Starborg[1], Sharon Brookes[1], Ignacio Palmero[1,3], Kevin Ryan[2], Eiji Hara[1,4], Karen H.Vousden[2] and Gordon Peters[1,5]

[1]Imperial Cancer Research Fund Laboratories, P.O. Box 123, 44 Lincoln's Inn Fields, London WC2A 3PX, UK, [2]NCI-Frederick Cancer Research and Development Center, Building 560, Room 22-96, West 7th Street, Frederick, MD 21702-1201, USA, [3]Centro Nacional de Biotecnologia, Campus Universidad Autonoma, Cantoblanco, 28049 Madrid, Spain and [4]Department of Preventive Medicine, 22nd Department of Surgery, Prefectural University of Medicine, Kawaramachi-Hirokoji, Kamigyo-ku, Kyoto 602 Japan

[5]Corresponding author
e-mail: peters@icrf.icnet.uk

The two distinct proteins encoded by the *CDKN2A* locus are specified by translating the common second exon in alternative reading frames. The product of the α transcript, p16^{INK4a}, is a recognized tumour suppressor that induces a G_1 cell cycle arrest by inhibiting the phosphorylation of the retinoblastoma protein by the cyclin-dependent kinases, CDK4 and CDK6. In contrast, the product of the human *CDKN2A* β transcript, p14^{ARF}, activates a p53 response manifest in elevated levels of MDM2 and p21^{CIP1} and cell cycle arrest in both G_1 and G_2/M. As a consequence, p14^{ARF}-induced cell cycle arrest is p53 dependent and can be abrogated by the co-expression of human papilloma virus E6 protein. p14^{ARF} acts by binding directly to MDM2, resulting in the stabilization of both p53 and MDM2. Conversely, p53 negatively regulates p14^{ARF} expression and there is an inverse correlation between p14^{ARF} expression and p53 function in human tumour cell lines. However, p14^{ARF} expression is not involved in the response to DNA damage. These results place p14^{ARF} in an independent pathway upstream of p53 and imply that *CDKN2A* encodes two proteins that are involved in tumour suppression.

Keywords: cell cycle/MDM2/p53 response/replicative senescence/tumour suppression

Introduction

The *CDKN2A* locus on human chromosome 9p21 (Kamb *et al*., 1994; Nobori *et al*., 1994) and the cognate loci on mouse chromosome 4 (Jiang *et al*., 1995; Quelle *et al*., 1995a) and rat chromosome 5 (Swafford *et al*., 1997) encode two distinct proteins translated from alternatively spliced mRNAs (see diagram in Figure 1A). The cyclin-dependent kinase inhibitor from which the locus takes its name (also known as p16^{INK4a}) is specified by an RNA comprising exons 1α, 2 and 3 (Serrano *et al*., 1993; Kamb *et al*., 1994; Nobori *et al*., 1994) referred to as the α transcript. The alternative product, designated ARF for 'alternative reading frame', is encoded by the slightly smaller β transcript that comprises exons 1β, 2 and 3 (Duro *et al*., 1995; Jiang *et al*., 1995; Mao *et al*., 1995; Quelle *et al*., 1995b; Stone *et al*., 1995b). The primary amino acid sequences of ARF and p16^{INK4a} are completely unrelated since they are produced by translating the common exon 2 sequences in different reading frames. Exon 1β bears no homology to exon 1α and, therefore, has the features of a distinct gene that has become inserted between the tandemly linked genes encoding p16^{INK4a} and its close relative p15^{INK4b} (reviewed in Larsen, 1996; Sidransky, 1996).

Most of the current information about ARF relates to the mouse homologue. The mouse β transcript was first noted during attempts to isolate cDNAs encoding mouse p16^{INK4a} (Quelle *et al*., 1995a) and subsequently shown to specify a protein of 169 amino acids, designated p19^{ARF}, that has no obvious relatives in the current databases (Quelle *et al*., 1995b). Quelle *et al*. went on to demonstrate that although mouse p19^{ARF} does not interfere directly with the function of cyclin-dependent kinases, it nevertheless invokes a cell cycle arrest when ectopically expressed in rodent cells (Quelle *et al*., 1995b). The most striking facet of the cell cycle arrest is the accumulation of cells with both a G_1 and G_2/M DNA content, with apparent exclusion of cells in S-phase. It was also noted that the levels of p19^{ARF} were generally higher in cells that had sustained mutations in the p53 tumour suppressor gene or in which p53 had been functionally compromised by overexpression of MDM2 (Quelle *et al*., 1995b).

Much less is known about the human equivalent of p19^{ARF}. The sequence of the human *CDKN2A* exon 1β was originally deduced from a combination of genomic DNA analysis, cDNA cloning and PCR-based approaches (Duro *et al*., 1995; Mao *et al*., 1995; Stone *et al*., 1995b). In the genomic DNA, the open reading frame continues for some distance upstream of the ATG that aligns with the start of the mouse p19^{ARF}-coding sequence. However, as this ATG is in a favourable context for translation initiation and is the first ATG in the presumptive transcript (Mao *et al*., 1995; Stone *et al*., 1995b), it is generally assumed that the human protein starts at this point. The encoded protein would therefore be predicted to comprise 132 amino acids with a molecular weight of 13 902 Da (see Figure 1B) and, by analogy to the corresponding mouse protein (p19^{ARF}), we refer to the human homologue as p14^{ARF} (Duro *et al*., 1995; Jiang *et al*., 1995; Mao *et al*., 1995; Quelle *et al*., 1995b; Stone *et al*., 1995b). The mouse and human proteins show only 50% identity over the region of overlap (Figure 1B), but transfection experiments have indicated that a cDNA representing the human β transcript can also induce a cell cycle arrest (Liggett *et al*., 1996; Arap *et al*., 1997).

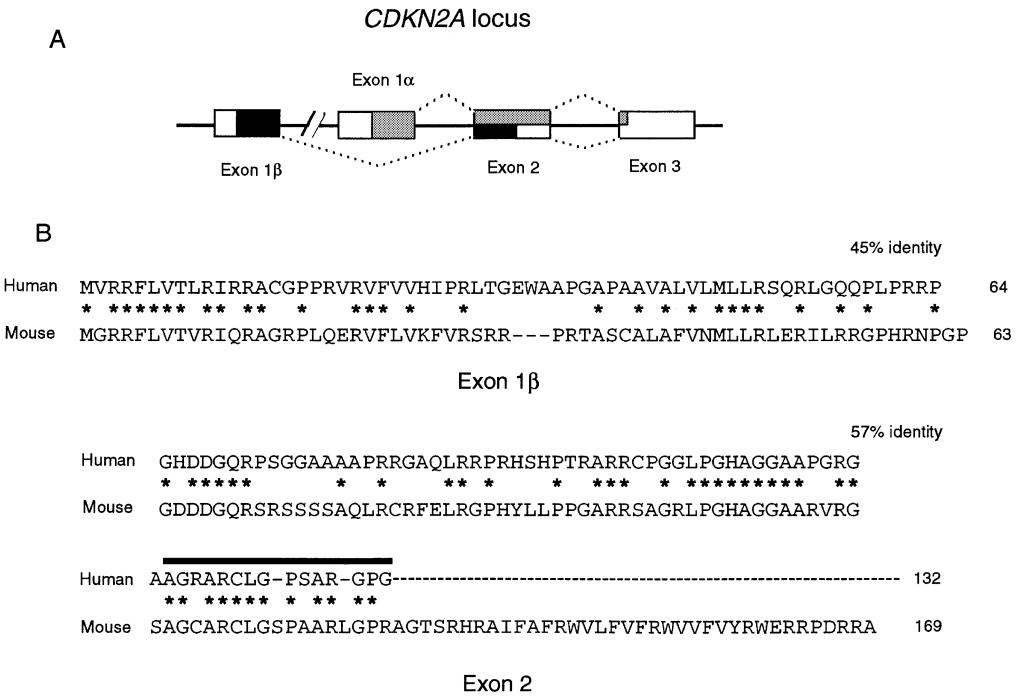

Fig. 1. Organization of the *CDKN2A* locus and sequence of $p14^{ARF}$. The genomic organization of the human *CDKN2A* gene is depicted in (**A**), with exons represented by boxes and coding domains by shading. The sequences encoding $p16^{INK4a}$ are in grey and those encoding $p14^{ARF}$ in black. (**B**) The amino acid sequences of human $p14^{ARF}$ and mouse $p19^{ARF}$ are shown in single letter code and split into exon 1β- and exon 2-encoded domains. The percentage identity in each exon is indicated. Identical residues are indicated by asterisks, and a gap has been introduced to maximize regional alignment.

The functional characterization of ARF has understandably been influenced by the approaches taken to study $p16^{INK4a}$ and its relatives which bind directly and specifically to the cyclin-dependent kinases CDK4 and CDK6, thereby inhibiting their ability to promote cell cycle progression via the phosphorylation of the retinoblastoma gene product, pRb (Sherr and Roberts, 1995; Weinberg, 1995; Sherr, 1996; Ruas and Peters, 1998). Thus, ectopic expression of $p16^{INK4a}$ or $p15^{INK4b}$ causes cells to accumulate with a G_0/G_1 DNA content, but cells that lack functional pRb are resistant to these effects (Guan *et al*., 1994; Okamoto *et al*., 1994; Koh *et al*., 1995; Lukas *et al*., 1995; Medema *et al*., 1995; Stone *et al*., 1995a). Conversely, cells that lack INK4 function are likely to have a proliferative advantage, and $p16^{INK4a}$ is now recognized as a major tumour suppressor implicated in a wide variety of tumour types (reviewed in Sherr, 1996; Ruas and Peters, 1998). Significantly, both the α transcript and $p16^{INK4a}$ accumulate when primary cells are propagated in tissue culture, suggesting that $p16^{INK4a}$ may participate in the G_1 arrest associated with replicative senescence (Alcorta *et al*., 1996; Hara *et al*., 1996; Loughran *et al*., 1996; Reznikoff *et al*., 1996; Wong and Riabowol, 1996; Palmero *et al*., 1997; Zindy *et al*., 1997). As well as explaining why $p16^{INK4a}$, rather than other members of the INK4 family, acts as a tumour suppressor, a role in senescence would account for the higher frequency of $p16^{INK4a}$ alterations noted in tumour cell lines as opposed to primary tumours (Cairns *et al*., 1994; Spruck *et al*., 1994), since there would be a strong selection against the expression of $p16^{INK4a}$ during the establishment of immortal clones.

Immortalization of human cells is facilitated by disruption of both pRb- and p53-dependent mechanisms (Shay and Wright, 1989; Wright *et al*., 1989; Hara *et al*., 1991; Shay *et al*., 1991a). Whereas the accumulation of $p16^{INK4a}$ with population doublings probably accounts for the pRb-linked mechanism, the p53 dependence is presumably associated with the accumulation of the $p21^{CIP1}$ CDK inhibitor (Noda *et al*., 1994; Alcorta *et al*., 1996). Through its ability to inhibit G_1-specific cyclin-dependent kinase complexes and to bind to proliferating cell nuclear antigen (PCNA), $p21^{CIP1}$ is believed to be a major executor of the p53-dependent cell cycle arrest that occurs in response to DNA damage (Brugarolas *et al*., 1995; Deng *et al*., 1995; reviewed in Sherr and Roberts, 1995; Levine, 1997). It has also been implicated directly in senescence by experiments showing that targeted disruption of $p21^{CIP1}$ can extend the lifespan of human diploid fibroblasts (Brown *et al*., 1997) and that activation of the *RAS–RAF* signalling pathway can elicit a cell cycle arrest via the up-regulation of $p21^{CIP1}$ (Lloyd *et al*., 1997; Sewing *et al*., 1997; Woods *et al*., 1997). However, the relative contributions of $p21^{CIP1}$ and $p16^{INK4a}$ in senescence have yet to be evaluated fully, and fibroblasts derived from mice with targeted disruptions of either gene fail to undergo senescence (Deng *et al*., 1995; Serrano *et al*., 1996). Interestingly, recent evidence suggests that this is also true for mouse cells with a specific disruption of exon 1β, further complicating the interpretation (Kamijo *et al*., 1997).

Since there are inherent differences in the immortalization frequencies of mouse and human cells and presumably in the underlying mechanisms, we considered it important to characterize the expression patterns and biological properties of the human homologue of ARF.

Like its mouse counterpart, human $p14^{ARF}$ is located in nuclear speckles in asynchronously growing cells, and ectopic expression of $p14^{ARF}$ causes cells to accumulate with both a G_1 and G_2/M DNA content, in stark contrast to the arrest induced by $p16^{INK4a}$ in the same cells. Significantly, the arrest invoked by $p14^{ARF}$ is accompanied by up-regulation of p53, $p21^{CIP1}$ and MDM2, and p53-negative tumour cells or cells expressing the human papilloma virus (HPV) E6 protein are insensitive to the effects of $p14^{ARF}$. Activation of p53 by $p14^{ARF}$ appears to reflect a direct interaction between $p14^{ARF}$ and MDM2 that inhibits the MDM2-mediated degradation of p53. Elevated expression of $p14^{ARF}$ therefore leads to the accumulation of both MDM2 and p53 by affecting the balance between transcriptional activation and protein turnover. In turn, the expression of endogenous $p14^{ARF}$ is negatively regulated by p53, and we show that in a panel of human tumour cell lines there is an inverse correlation between $p14^{ARF}$ expression and p53 status that has parallels with the feedback loop observed between $p16^{INK4a}$ expression and pRb status in human cells (Li *et al*., 1994b; Hara *et al*., 1996; Palmero *et al*., 1997). However, there is no evidence that the β transcript is involved in a DNA damage response. We therefore favour a model in which $p14^{ARF}$ is a component of a separate pathway upstream of p53 such that targeted disruption of exon 1β is likely to reproduce some but not all of the phenotypic characteristics of p53-nullizygous mice. These results are discussed in relation to the possible role of ARF as a tumour suppressor.

Results

Detection of human $p14^{ARF}$

Using the known sequence to predict suitable primers, a cDNA corresponding to the human *CDKN2A* β transcript was generated by reverse transcription and PCR using RNA obtained from TIG3 human diploid fibroblasts. The DNA sequence predicts a protein of 132 amino acids that terminates prematurely compared with the mouse homologue (Figure 1B). Polyclonal antisera were generated against a synthetic peptide corresponding to the C-terminal 15 amino acids of human $p14^{ARF}$ and validated in a number ways. For example, the antisera were capable of immunoprecipitating [^{35}S]methionine-labelled $p14^{ARF}$ generated by coupled *in vitro* transcription and translation (not shown). In Western blots, the antisera detected a 14 kDa protein in cells that had been engineered to express the β cDNA under the control of an isopropyl-β-D-thiogalactopyranoside (IPTG)-inducible promoter (see below). Although the mouse protein migrates anomalously in SDS–PAGE, possibly due to the high arginine content (Quelle *et al*., 1995b), the shorter human protein migrates as expected at 14 kDa and is clearly distinguishable from $p16^{INK4a}$.

Following affinity purification on immobilized peptide, the antisera were able to detect endogenous $p14^{ARF}$ by immunofluorescence. As illustrated in Figure 2, staining of the 5637 bladder carcinoma cell line revealed a distinctive punctate pattern as well as staining of larger more diffuse bodies (Figure 2A). By direct comparison with phase contrast images, it is clear that these correspond to nucleoli (Figure 2C and D). The staining could be competed by excess peptide (Figure 2B) and was present in almost all cells (Figure 2E and F). Less distinct staining was noted in mitotic figures. A similar staining pattern was detected in U2OS cells that expressed inducible $p14^{ARF}$, and in these cells positive staining was dependent on the addition of IPTG (Figure 2G and H). This pattern of staining is virtually identical to that seen with mouse $p19^{ARF}$ (Quelle *et al*., 1995b) and has recently been described for the human protein in HeLa and HS27 cells (Della Valle *et al*., 1997).

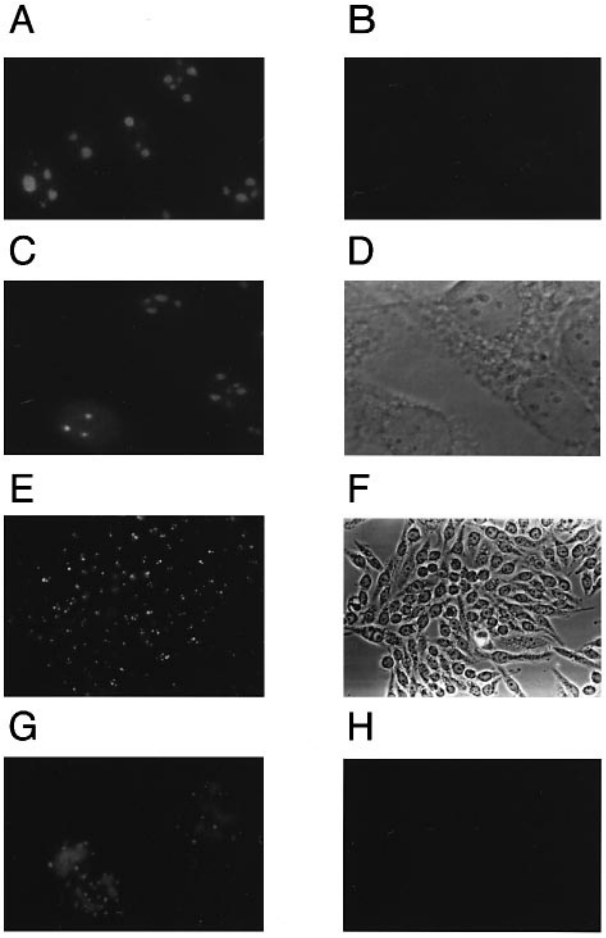

Fig. 2. Localization of $p14^{ARF}$ by immunofluorescence. Logarithmically growing monolayer cultures were fixed and stained with an affinity-purified polyclonal antiserum against the C-terminal 15 residues of human $p14^{ARF}$. (**A**) 5637 bladder carcinoma cells; (**B**) the same cells with the primary antibody pre-adsorbed against excess peptide antigen; (**C** and **D**) matching immunofluorescence and phase contrast images of 5637 cells; (**E** and **F**) the same cells at lower magnification; (**G**) U2OS cells expressing IPTG-inducible $p14^{ARF}$; (**H**) the same cells without IPTG induction. (A–D) and (G–H) were photographed at 100× magnification, whereas (E) and (F) were at 20× magnification.

Cell cycle arrest by inducible expression of $p14^{ARF}$

Mouse $p19^{ARF}$ has previously been shown to arrest cells in both G_1 and G_2/M phases when ectopically expressed using retroviral vectors (Quelle *et al*., 1995b), but the nature of the arrest elicited by human ARF has not been defined (Liggett *et al*., 1996; Arap *et al*., 1997). To address this issue and to compare directly the properties of $p14^{ARF}$ and $p16^{INK4a}$, the U2OS osteosarcoma cell line, which is wild-type for both p53 and pRb (Diller *et al*., 1990), was

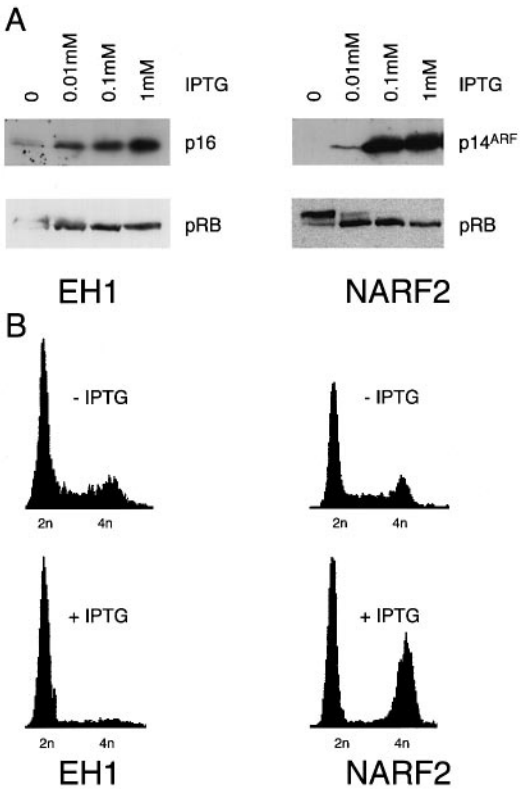

Fig. 3. Cell cycle arrest by inducible expression of $p14^{ARF}$ and $p16^{INK4a}$. (**A**) EH1 and NARF1 cells were treated with increasing amounts of IPTG as indicated, and the expression of $p16^{INK4a}$ and $p14^{ARF}$ monitored by immunoblotting. The same samples were also immunoblotted with an antibody to pRb to determine the extent of phosphorylation. (**B**) FACS profiles of EH1 and NARF1 cells either untreated or treated for 48 h with 1 mM IPTG.

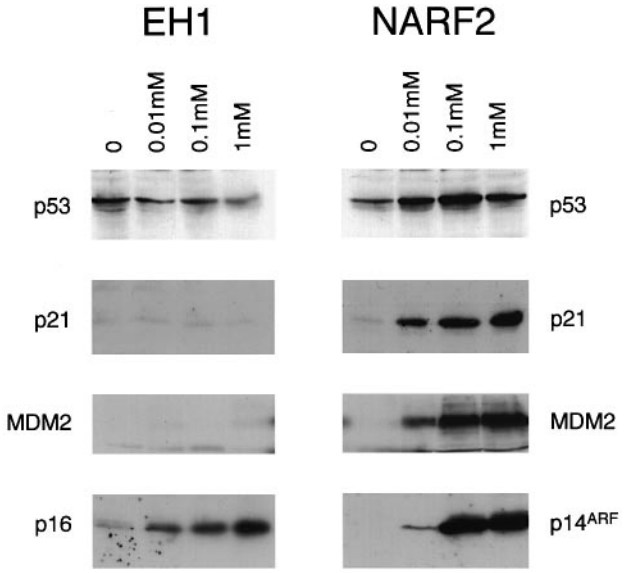

Fig. 4. Up-regulation of p53, $p21^{CIP1}$ and MDM2 by $p14^{ARF}$. Lysates prepared from EH1 and NARF1 cells treated with increasing doses of IPTG (as in Figure 3A) were immunoblotted with antibodies against p53, $p21^{CIP1}$ and MDM2, as indicated. The results for $p16^{INK4a}$ and $p14^{ARF}$ are reproduced from Figure 3A.

used to establish clones expressing regulatable forms of the corresponding cDNAs, based on the LAC SWITCH™ expression system (Stratagene). With the β cDNA, all six of the clonal lines tested (NARF1–NARF6) were found to express $p14^{ARF}$ upon addition of IPTG, whereas only two of the 30 lines transfected with the α cDNA (EH1 and EH2) showed inducible expression of $p16^{INK4a}$. In EH1 cells, the expression of $p16^{INK4a}$ was activated by as little as 0.01 mM IPTG and was maximal at between 0.3 and 1.0 mM IPTG, whereas the expression of $p14^{ARF}$ in NARF2 cells showed a steeper dose responsiveness, with maximal levels achieved with 0.1 mM IPTG (Figure 3A). Similar results were obtained with different clones, and two clones of $p14^{ARF}$-expressing cells, NARF1 and NARF2, were used interchangably in subsequent experiments. When the same cell lysates were immunoblotted for pRb protein (Figure 3A), it was clear that the phosphorylation of pRb, as judged by the presence of the more slowly migrating forms, was inhibited by the induction of either $p16^{INK4a}$ or $p14^{ARF}$. The degree of inhibition paralleled the dose responsiveness of $p16^{INK4a}$ and $p14^{ARF}$ expression (Figure 3A).

Since the inhibition of pRb phosphorylation is generally equated with a G_1-phase arrest, we also checked the cell cycle distribution of the inducible cell clones by propidium iodide staining and flow cytometry. As shown in Figure 3B, asynchronously growing EH1 and NARF2 cells had a normal cell cycle profile, with cells distributed in the G_1, S and G_2/M fractions. Upon addition of 1 mM IPTG, the EH1 cells, expressing inducible $p16^{INK4a}$, arrested with a G_1 DNA content as expected. In contrast, the NARF2 cells expressing inducible $p14^{ARF}$ accumulated in both the G_1 and G_2/M phases (Figure 3B).

More detailed analyses were performed to determine the time scale, dose responsiveness and reversibility of the arrests imposed by either $p14^{ARF}$ or $p16^{INK4a}$. Changes in cell cycle profiles were apparent as early as 6 h after IPTG addition and were essentially maximal after 24 h in the case of $p14^{ARF}$, whereas the proportion of $p16^{INK4a}$-expressing cells in G_1 continued to increase up to 48 h (not shown). The effects were more pronounced at higher concentrations of IPTG, reflecting the dose responsiveness of $p14^{ARF}$ or $p16^{INK4a}$ induction, and in both cases cells treated with 1 mM IPTG for 48 h were able to resume normal cycling upon removal of the inducer (not shown).

Activation of p53 and p21 by ectopic expression of $p14^{ARF}$

The ability of $p14^{ARF}$ to arrest cells in the G_1 and G_2/M phases of the cycle suggested that the effects might be mediated via p53 (Agarwal *et al.*, 1995). Lysates prepared from NARF2 and EH1 cells treated with increasing concentrations of IPTG (as in Figure 3A) were immunoblotted with antibodies against p53, $p21^{CIP1}$ and MDM2. As shown in Figure 4A, the levels of p53 itself were clearly increased upon induction of $p14^{ARF}$ in NARF2 cells, but there was no obvious effect on p53 upon induction of $p16^{INK4a}$ in EH1 cells. More dramatic induction by $p14^{ARF}$ was observed for $p21^{CIP1}$ and MDM2, both of which are targets for transcriptional activation by p53 (Barak *et al.*, 1993; El-Deiry *et al.*, 1993; Wu *et al.*, 1993), and the effects were broadly in line with the dose dependence of $p14^{ARF}$ expression. No changes in $p21^{CIP1}$ and MDM2 levels were observed in EH1 cells. These data clearly imply that elevated levels of $p14^{ARF}$ cause the functional activation of p53.

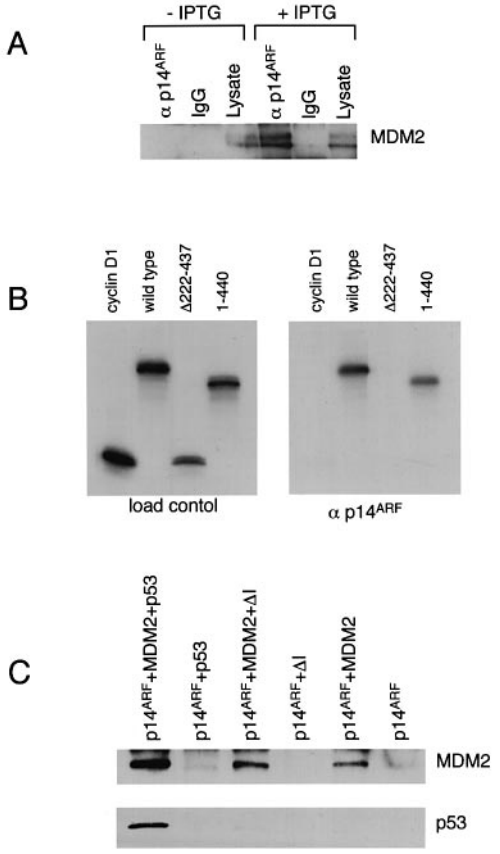

Fig. 5. Physical interaction of $p14^{ARF}$ with MDM2 and p53. (**A**) Lysates prepared from NARF1 cells with and without addition of 1 mM IPTG were either analysed directly (Lysate) or immunoprecipitated with $p14^{ARF}$ antiserum or the pre-immune control (IgG) and immunoblotted for MDM2. (**B**) *In vitro* binding of $p14^{ARF}$ and MDM2. The left hand panel shows the individual [^{35}S]methionine-labelled translation products and the right hand panel shows the co-immunoprecipitation of labelled products with $p14^{ARF}$ antiserum. Wild-type MDM2 and a form lacking the C-terminal 51 residues (1–440) associated with $p14^{ARF}$ in this assay, whereas the Δ222–437 mutant did not. (**C**) Co-precipitation of $p14^{ARF}$, p53 and MDM2 from transiently transfected SAOS2 cells with antiserum against $p14^{ARF}$. The efficient immunoprecipitation of p53 depended on the co-expression of MDM2 and was not apparent with a deleted form of p53 (ΔI) that lacks the MDM2-binding site.

Direct binding of $p14^{ARF}$ and MDM2

In other settings, such as the response to DNA damage, a rapid increase in p53 levels is brought about through stabilization of the protein. In undamaged cells, the p53 protein is turned over rapidly at least in part through interaction with MDM2 which targets p53 for ubiquitination and proteasome-mediated degradation (Haupt *et al*., 1997; Kubbutat *et al*., 1997). We therefore asked whether the ability of $p14^{ARF}$ to activate a p53 response in NARF cells occurred via a physical interaction with either MDM2 or p53. When $p14^{ARF}$ immunoprecipitates from NARF cells were immunoblotted with a monoclonal antibody against MDM2, clear evidence for co-precipitation was obtained, specifically in cells that had been treated with IPTG (Figure 5A). This interaction was investigated further *in vitro* using labelled proteins expressed by coupled transcription and translation in reticulocyte lysates. In this direct binding assay, wild-type MDM2 and a mutant form lacking the C-terminal 51 amino acids (1–440) were co-precipitated efficiently with $p14^{ARF}$ (Figure 5B). In contrast, the cyclin D1 control and a mutant form of MDM2 lacking residues 222–437 did not bind efficiently to $p14^{ARF}$ under these conditions. Note that the Δ222–437 mutant did show some residual degree of binding when the corresponding plasmid constructs were co-expressed in U2OS cells (data not shown). However, attempts to map the $p14^{ARF}$-binding domain on MDM2 in this way have so far produced equivocal results.

The transient co-transfection assay was also used to determine whether $p14^{ARF}$ could form ternary complexes with p53 and MDM2. SAOS2 cells, which lack endogenous p53, were transfected with various combinations of plasmids encoding $p14^{ARF}$, MDM2, p53 or a form of p53 (ΔI) lacking conserved box I that is incapable of binding MDM2 (Marston *et al*., 1994; Kubbutat *et al*., 1997). To avoid potential apoptotic effects, both forms of p53 used in this experiment were also deleted for conserved box II (kindly provided by M.Ashcroft). The $p14^{ARF}$ immunoprecipitates were then immunoblotted for p53 and MDM2. From these data, it was clear that $p14^{ARF}$ was capable of forming a three-way complex with p53 and MDM2, and that the co-precipitation of p53 was absolutely dependent on the presence of MDM2 (Figure 5C). The ΔI mutant of p53 did not enter a ternary complex with $p14^{ARF}$ presumably because of its inability to bind MDM2.

Stabilization of p53 by expression of $p14^{ARF}$

We next asked whether the association of $p14^{ARF}$ with MDM2 had any effect on its ability to promote the degradation of p53. As shown previously (Kubbutat *et al*., 1997), co-transfection of MDM2 leads to a dose-dependent reduction in the amount of p53 protein detectable after 24 h (Figure 6A). This MDM2-induced turnover of p53 was completely inhibited by co-transfection of $p14^{ARF}$. Similar effects were observed with mouse and human MDM2 and in U2OS and SAOS2 cells (data not shown). Significantly, there was also a marked accumulation of MDM2 in the $p14^{ARF}$-transfected cells, analogous to the effects seen with inducible $p14^{ARF}$ in NARF cells. In the transiently transfected cells, the increased expression of MDM2 cannot be attributed to transcriptional activation by p53 since it is being expressed from a heterologous promoter. Moreover, the LLnL proteasome inhibitor, which can protect p53 from MDM2-mediated degradation (Kubbutat *et al*., 1997), had no additional effect on p53 levels over those attributable to co-expression of $p14^{ARF}$ (Figure 6B). Thus, $p14^{ARF}$ appears to stabilize both p53 and MDM2.

To explore further the effects of $p14^{ARF}$ on MDM2, co-transfections were carried out with two mutant forms of MDM2 (1–440 and 6–339) that lack the C-terminal domain and are therefore impaired in their ability to target p53 for ubiquitin-mediated degradation (M.Kubbutat and K.H.Vousden, in preparation). Both mutants were stabilized by $p14^{ARF}$ in the absence of co-transfected p53 (Figure 6C). Moreover, co-expression of the E6 protein of HPV16, which independently targets p53 for degradation (Scheffner *et al*., 1990), did not diminish the effects of $p14^{ARF}$ on MDM2 levels (Figure 6D).

p53 dependence of the $p14^{ARF}$-mediated arrest

The ability of $p14^{ARF}$ to activate the p53-dependent expression of $p21^{CIP1}$ suggested that the cell cycle arrest

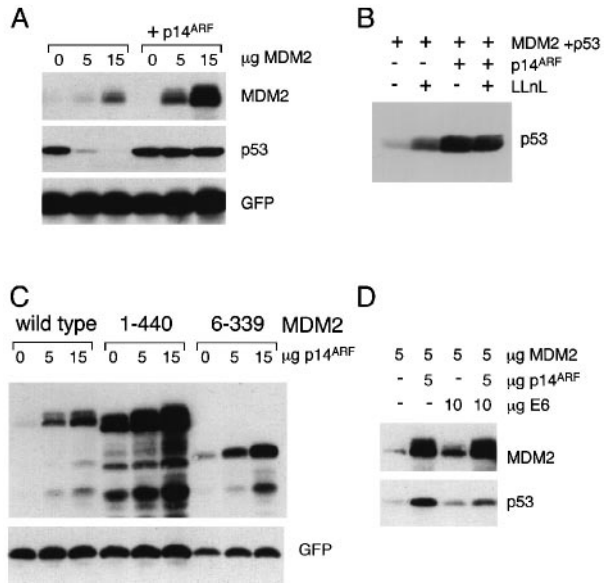

Fig. 6. Functional interaction of $p14^{ARF}$ with MDM2 and p53. (**A**) U2OS cells were transfected with plasmids encoding p53, MDM2 and $p14^{ARF}$ as indicated, and p53 and MDM2 levels were analysed by immunoblotting (Kubbutat *et al*., 1997). Co-transfection of 5 µg of $p14^{ARF}$ vector efficiently overcame the ability of MDM2 to induce degradation of p53 and resulted in the stabilization of MDM2. The lower panel shows the immunodetection of green fluorescent protein (GFP) which was included as a control for transfection efficiency. (**B**) An analogous experiment was performed in the presence or absence of the proteasome inhibitor LLnL. In the presence of $p14^{ARF}$, LLnL failed to cause additional stabilization of p53. (**C**) In the absence of exogenous p53, increasing amounts of $p14^{ARF}$ (0, 5 and 15 µg) caused the accumulation of wild-type MDM2 as well as two mutant forms (1–440 and 6–339) lacking the C-terminal ring finger domain. GFP was used as a control for transfection efficiency. (**D**) A similar experiment was performed in the presence or absence of HPV16 E6. Co-expression of $p14^{ARF}$ caused an increase in the amount of MDM2 irrespective of the presence of E6.

imposed by $p14^{ARF}$ would depend on the presence of functional p53, in the same way that the arrest imposed by $p16^{INK4a}$ is dependent on functional pRb (Koh *et al*., 1995; Lukas *et al*., 1995; Medema *et al*., 1995). We therefore tested this prediction in a number of different ways. The most direct assay was to transfect established human tumour cell lines of known p53 and pRb status with pcDNA3-based plasmids capable of expressing the *CDKN2A* α and β RNAs from a cytomegalovirus (CMV) promoter. The cells were co-transfected with a plasmid encoding the CD20 cell surface marker and, 48–60 h post-transfection, the proportions of the CD20-expressing cells in different phases of the cell cycle were determined by dual-colour flow cytometry (van den Heuvel and Harlow, 1993). In this transient assay, the G_2 arrest associated with $p14^{ARF}$ or $p21^{CIP1}$ expression is not apparent and the results were therefore interpreted as the relative increase in the proportion of cells in G_1.

The three representative cell lines used for these analyses were the the breast cancer line MCF7, which is wild-type for both pRb and p53 function (pRb+/p53+), the lung carcinoma line H1299, which is pRb+/p53–, and the osteosarcoma line SAOS2, which is pRb–/p53–. In MCF7 cells, transient expression of $p14^{ARF}$, $p16^{INK4a}$ and $p21^{CIP1}$ caused equivalent increases in the G_1 population (~35%) compared with the vector-only control (pcDNA3), confirming that the expressed sequences were functional (Figure 7A). However, $p14^{ARF}$ did not induce a growth arrest in either H1299 or SAOS2 cells, both of which lack p53. This contrasts with $p16^{INK4a}$ which was able to arrest the pRb-positive H1299 cells but not the pRb-negative SAOS2 cells, and $p21^{CIP1}$ which was effective on all three cell types, presumably because of its ability to inhibit cyclin-dependent kinases that function downstream of pRb (Harper *et al*., 1995; Medema *et al*., 1995; Lukas *et al*., 1996; Mann and Jones, 1996). Immunoblotting of the transfected cell lysates confirmed that the three cell lines were expressing comparable levels of $p14^{ARF}$ and, as expected, only the p53-positive cell line MCF7 showed the concomitant induction of $p21^{CIP1}$ and p53 (Figure 7B). Note that H1299 cells express a significant level of $p21^{CIP1}$ that is detectable on longer exposures, but that this basal level is not affected by expression of $p14^{ARF}$.

To confirm further the p53 dependence of the $p14^{ARF}$-mediated arrest, MCF7 cells were co-transfected with pcDNA3-ARF and a vector encoding the the HPV16 E6 protein. As shown in Figure 7C, co-expression of E6 prevented the $p14^{ARF}$-mediated arrest in MCF7 cells but had no effect on the arrest elicited by transient transfection of $p16^{INK4a}$. As anticipated, the presence of E6 abrogated the effects of $p14^{ARF}$ on the endogenous $p21^{CIP1}$ and p53 levels in the transfected cells (Figure 7D). Significantly, a plasmid designed to express only the exon 1β-encoded sequences, designated N65ARF, was also capable of inducing a G_1 arrest in transiently transfected MCF7 cells, indicating that the exon 2-encoded sequences in $p14^{ARF}$ are not essential for its ability to activate p53 (Figure 7E). Similar conclusions were drawn for the mouse homologue (Quelle *et al*., 1997).

p53 dependence of $p14^{ARF}$-induced arrest in diploid fibroblasts

To avoid any confounding effects from additional genetic alterations that might be present in established tumour cell lines, we also used the HPV16 E6 protein to interfere with p53 function in primary human diploid fibroblasts (HDFs). The TIG3 strain of HDFs that had been rendered sensitive to ecotropic murine retroviruses by expression of the mouse basic amino acid transporter (McConnell *et al*., 1998) were infected with $p14^{ARF}$- and/or E6-encoding retrovirus in the pBABE-hygro and pBABE-puro vectors, respectively. Pools of infected cells were then recovered by appropriate drug selection and compared in a cell proliferation assay. The TIG3 cells infected with $p14^{ARF}$-encoding virus showed a markedly reduced proliferative capacity compared with the vector-only controls, but the effect was relieved by co-infection with E6 (Figure 8A). In the continued presence of serum, the $p14^{ARF}$-infected cells adopted phenotypic characteristics typical of replicative senescence, such as increased size and the expression of senescence-associated β-galactosidase (SA-β-gal) activity (Dimri *et al*., 1995). We have shown previously that ectopic expression of either $p21^{CIP1}$ or $p16^{INK4a}$ can elicit similar effects in early passage TIG3 cells (McConnell *et al*., 1998). Co-infection with a virus encoding E6 markedly reduced the proportion of cells staining positively for SA-β-gal activity (Figure 8B).

Relationship of $p14^{ARF}$ expression to p53 status

Previously we have shown that TIG3 cells transformed by SV40 T-Ag (SVts8) express elevated levels of the

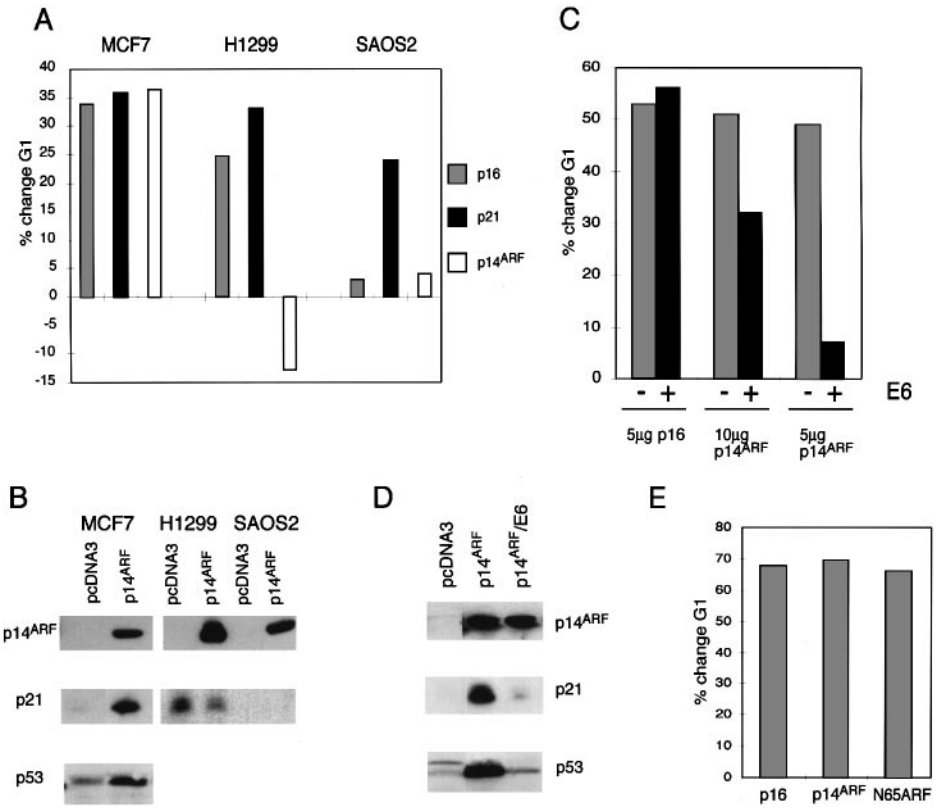

Fig. 7. p53 dependence of the $p14^{ARF}$-induced cell cycle arrest. (**A**) MCF7, H1299 and SAOS2 cells were co-transfected with vectors encoding the cell surface marker CD20 plus $p16^{INK4a}$, $p21^{CIP1}$ or $p14^{ARF}$ as indicated. After 48 h, the relative DNA contents of the CD20-positive cells were assessed by dual-colour flow cytometry. The results are plotted as the percentage change in the G_1 fraction relative to cells transfected with vector alone. Only the p53-positive MCF7 cells were arrested by $p14^{ARF}$ whereas $p21^{CIP1}$ affected all cells and the $p16^{INK4a}$ arrest was pRb dependent. (**B**) Immunoblotting of the transiently transfected cell lysates to confirm expression of $p14^{ARF}$. Note the concomitant up-regulation of $p21^{CIP1}$ and p53 only occurred in the p53-positive MCF7 cells. (**C**) MCF7 cells stably expressing HPV16 E6 protein were shown to be partially resistant to the cell cycle arrest imposed by transiently transfected $p14^{ARF}$ but still responded to $p16^{INK4a}$. (**D**) Confirmation that the cells in (C) were expressing equivalent levels of $p14^{ARF}$ but that $p21^{CIP1}$ and p53 were not induced in the presence of E6. (**E**) Transfection of exon 1β sequences alone (N65ARF) induced a G_1 arrest in MCF7 cells that was indistinguishable from the arrest imposed by full-length $p14^{ARF}$.

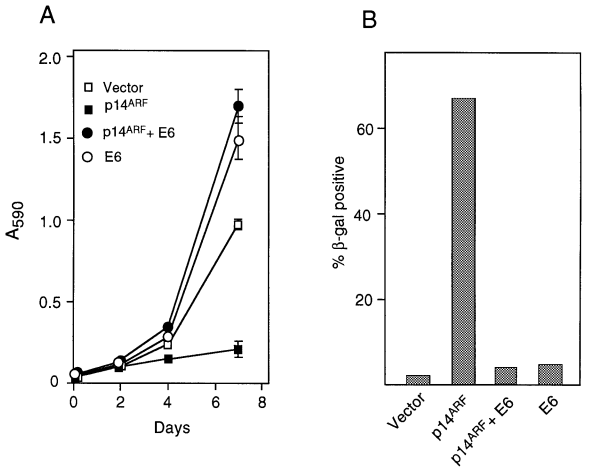

Fig. 8. Abrogation of $p14^{ARF}$-induced growth arrest by HPV16 E6. (**A**) TIG3 primary human fibroblasts and the same cells infected with a retrovirus encoding E6 (puromycin resistant) were infected with recombinant retroviruses encoding $p14^{ARF}$ (hygromycin resistant) and pools of infected cells were selected over 7 days. Equal numbers of cells were then seeded in 24-well dishes and cell proliferation was monitored over the following 7 days. (**B**) At 15 days post-infection, cells were stained for SA-β-gal activity (Dimri *et al*., 1995). The proportion of SA-β-gal-positive cells in pools infected with $p14^{ARF}$ virus was markedly reduced by co-infection of E6.

CDKN2A β transcript, suggesting a link with the status of either the p53 or pRb genes (Hara *et al*., 1996). Indeed, in nuclear run-on experiments, it was possible to demonstrate modulation of exon 1β transcription by a temperature-sensitive form of SV40 T-Ag (Hara *et al*., 1996). These data did not distinguish between effects related to pRb or p53, both of which are targeted by SV40 T-Ag, but the availability of TIG3 cells infected with an E6 retrovirus enabled us to clarify this issue. In line with the previous findings, SVts8 cells grown at the permissive temperature for T-Ag function contained readily detectable levels of $p14^{ARF}$, and the same was true for TIG3 cells expressing HPV16 E6 (Figure 9A). In contrast, little if any $p14^{ARF}$ could be observed in the control TIG3 cells (Figure 9A). Conversely, the TIG3 cells expressing SV40T-Ag and HPV16 E6 showed the expected down-regulation of endogenous $p21^{CIP1}$ levels.

Up-regulation of $p14^{ARF}$ expression by E6 would be consistent with a negative feedback loop in which p53 represses the expression of the *CDKN2A* β transcript. To explore this possibility further, we examined $p14^{ARF}$ levels in SAOS2 cells that had been engineered to express wild-type p53 under the control of an inducible promoter or that had been stably transfected with a plasmid encoding a temperature-sensitive form p53 (V143A). In both settings, activation of p53 resulted in markedly decreased expres-

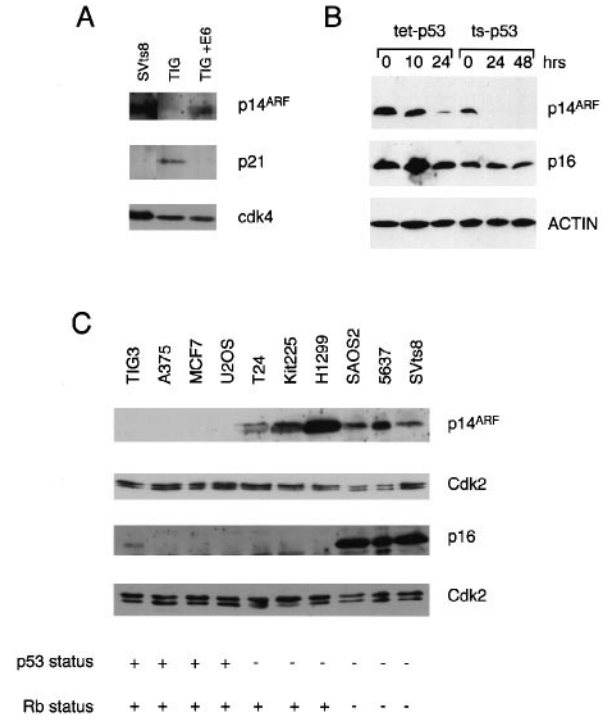

Fig. 9. Inverse correlation between $p14^{ARF}$ expression and p53 status. (**A**) TIG3 cells infected with empty vector or with E6-encoding retrovirus were analysed for expression of $p14^{ARF}$. The level of $p14^{ARF}$ observed in E6-expressing cells approximated that observed in SVts8 cells (TIG3 cells transformed by temperature-sensitive SV40 T-Ag) grown at the permissive temperature. The same lysates were immunoblotted for CDK4, as a load control, and for $p21^{CIP1}$ to confirm the effects of E6 and T-Ag on endogenous $p21^{CIP1}$ levels. (**B**) SAOS2 cells stably transfected with tetracycline-regulated p53 or with temperature-sensitive p53 were immunoblotted for $p14^{ARF}$ at the indicated times after tetracycline addition or switch to the permissive temperature. Whereas $p14^{ARF}$ levels were markedly decreased, there was no effect on the $p16^{INK4a}$ and actin levels. (**C**) Equivalent amounts (20 μg) of total cellular protein from logarithmically growing cultures of the indicated cells were fractionated in a 15% polyacrylamide gel and immunoblotted with antisera against $p14^{ARF}$, $p16^{INK4a}$ and CDK2. The CDK2 signal served as a loading control. The results with additional cell lines are summarized in Table I.

sion of $p14^{ARF}$ manifest 24 h after tetracyline addition or temperature shift (Figure 9B). These results establish clear evidence for the proposed feedback loop.

Inverse correlation of $p14^{ARF}$ expression and p53 status in human cell lines

The existence of this feedback loop, together with previous observations on mouse ARF expression, suggested that there should be an inverse correlation between $p14^{ARF}$ and p53 status in human tumour cell lines. To investigate this possibility, a selection of human cell lines with known p53 and pRb status was analysed for expression of the β transcript and for $p14^{ARF}$. In all cases tested, there was a complete concordance between the presence of the β transcript and a detectable level of $p14^{ARF}$ by immunoblotting (Table I). Significantly, $p14^{ARF}$ was only detected in cell lines that had a defective p53 gene (Figure 9C). Notable examples include the H1299 lung carcinoma line (p53–/pRb+), the 5637 bladder carcinoma line (p53–/pRb–) and the interleukin-2 (IL-2)-dependent T-cell line Kit225; although the latter cells may have wild-type p53, as judged by lack of reactivity with the monoclonal

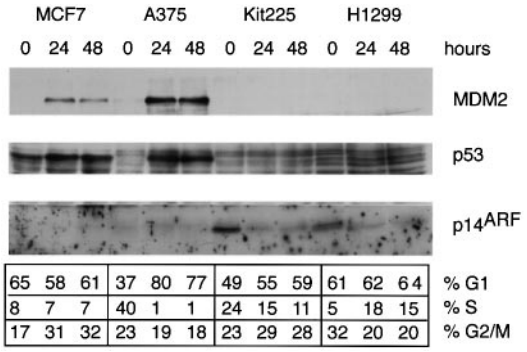

Fig. 10. $p14^{ARF}$ expression is independent of DNA damage. MCF7, A375, Kit225 and H1299 cells were treated with 5 nM actinomycin D for the indicated times. Cell lysates were then analysed for expression of MDM2, p53 and $p14^{ARF}$ as indicated. (Bottom panel) Samples of the treated cells were analysed by flow cytometry to determine the proportion of cells in G_1, S and G_2/M phases. Actinomycin D treatment invoked a p53 response in MCF7 and A375 cells despite the absence of exon 1β sequences, whereas Kit225 and H1299 cells (both p53-negative) showed no p53 response and no activation of $p14^{ARF}$.

Table I. Expression of $p14^{ARF}$ and $p16^{INK4a}$ relative to p53 and pRb status

Cell line	Cell type	RB	p53	$p16^{INK4a}$	$p14^{ARF}$
A375	melanoma	+	+	–	del
H1299	lung	+	–	+	+++
H596	lung	–	–	+++	+++
T24	bladder	+	–	meth	+
5637	bladder	–	–	+++	+++
MDA MB468	breast	–	–	+++	+
BT549	breast	–	–	+++	+++
MCF7	breast	+	+	del	–
MDA MB231	breast	+	–	del	del
SAOS2	osteosarcoma	–	–	+++	+
U20S	osteosarcoma	+	+	meth	–
C33A	cervical	–	–	+++	+++
CEM	T-lymphocyte	+	–	del	del
Kit225	T-lymphocyte	+	–	meth	+++
WI38	fibroblast	+	+	+	+/–
VA13	SV40-fibro	–	–	+++	+
TIG3	fibroblast	+	+	+	+/–
SVts8	SV40-fibro	–	–	+++	+

This table summarizes the expression patterns of $p16^{INK4a}$ and $p14^{ARF}$ in the indicated tumour cell lines and primary fibroblast strains. The relative intensities of the signals are indicated as +++, + and +/–. The latter signifies a situation in which low levels of β RNA have been observed but the protein is below the level of detection with the available antisera. del refers to situations in which the genomic DNA has been deleted and meth where exon 1α has been transcriptionally silenced by methylation. Apart from Kit225 (see text), the status of pRb and p53 in these cell lines is based on published information (see, for example, Horowitz *et al*., 1990; Bates *et al*., 1994b; Hainaut *et al*., 1997).

antibody pAb240, they appear to be operationally p53-defective as judged by their response to DNA damage (see Figure 10). No $p14^{ARF}$ was detected in the p53-positive lines, such as U2OS, MCF7 and A375, but the latter cell line represents one of the rare situations in which exon 1β is deleted but exons 1α, 2 and 3 of $p16^{INK4a}$ are spared (Stone *et al*., 1995b), whereas MCF7 cells present the interesting situation in which exon 1β is present but exons 1α, 2 and 3 are deleted (Kamb *et al*., 1994). To date, we have not identified a p53-positive tumour cell line in which $p14^{ARF}$ is detectable with the available antisera.

The patterns of $p14^{ARF}$ expression were quite distinct from those of $p16^{INK4a}$ which, as expected from previous work, showed an inverse correlation with the status of pRb (Figure 9C and Table I). Whereas all pRb-negative cells expressed high levels of $p16^{INK4a}$, no expression was detected in pRb-positive cell lines such as Kit225, T24 and U2OS, in which exon 1α is methylated (unpublished observations) or in CEM and MCF7 where the gene has been homozygously deleted.

$p14^{ARF}$ expression is not linked to DNA damage

Having established that $p14^{ARF}$ is capable of activating p53 and may itself be regulated by p53, we were interested in determining what other signals might impact on the expression of $p14^{ARF}$. A variety of different signals have been shown to activate p53-mediated responses, including DNA damage, hypoxia, oncogenic stimulation and senescence (Bates and Vousden, 1996). Several of the cell lines surveyed in Table I as well as primary diploid fibroblasts were therefore tested for their responsiveness to actinomycin D, a chemotherapeutic drug which at low doses elicits a strong p53 response. We were unable to detect any $p14^{ARF}$ in fibroblasts before or after treatment with actinomycin D (data not shown). Conversely, the MCF7 and A375 cell lines showed the expected up-regulation of p53 upon treatment with actinomycin D despite the absence of $p14^{ARF}$, whereas the Kit225 and H1299 cell lines, which express relatively high levels of $p14^{ARF}$, showed no discernible p53 response (Figure 10). Although the low levels of actinomycin D used in these experiments should not block transcription, there was a noticeable decrease in $p14^{ARF}$ levels in Kit225 and H1299 cells. The origin of this effect remains unclear and is the subject of ongoing research.

Discussion

The data we present here reaffirm the existence and importance of the alternative product encoded by the mammalian *CDKN2A* locus by providing unequivocal evidence for the presence of the human homologue, $p14^{ARF}$, in the nuclei of human tumour cells and by linking its function to that of the p53 tumour suppressor. Like its mouse counterpart, human $p14^{ARF}$ has the ability to elicit a p53 response, manifest in the increased expression of both $p21^{CIP1}$ and MDM2 (Figure 3A; Kamijo *et al*., 1997) and resulting in a distinctive cell cycle arrest in both the G_1 and G_2/M phases (Figure 3B; Quelle *et al*., 1995b). This arrest is consistent with the recent demonstration that inducible expression of $p21^{CIP1}$ can itself elicit a G_1 and G_2 arrest (Bates *et al*., 1998; Cayrol *et al*., 1998; Medema *et al*., 1998; Niculescu *et al*., 1998) as well as a body of data implicating p53 and $p21^{CIP1}$ in G_2/M-related events (Li *et al*., 1994a; Agarwal *et al*., 1995; Cross *et al*., 1995; Stewart *et al*., 1995; Fukasawa *et al*., 1996). A likely explanation is the proven ability of $p21^{CIP1}$ to inhibit cyclin B–CDK1 activity as well as cyclin–CDK complexes operating in G_1 and S phases of the cell cycle (Bates *et al*., 1998; Medema *et al*., 1998). This contrasts with the effects of $p16^{INK4a}$ which is specific for complexes containing CDK4 and CDK6 and induces an exclusively G_1 arrest (Figure 3B; Koh *et al*., 1995; Lukas *et al*., 1995; Medema *et al*., 1995). The involvement of $p21^{CIP1}$ would also explain the fact that unlike $p16^{INK4a}$, $p14^{ARF}$ can arrest both pRb-positive and pRb-negative cells (Figure 7; Liggett *et al*., 1996).

In seeking a mechanism for the effects of $p14^{ARF}$ on p53, we showed that $p14^{ARF}$ can interact directly with the MDM2 protein, both *in vivo* and *in vitro* (Figure 5), consistent with recently published data from other groups (Pomerantz *et al*., 1998; Zhang *et al*., 1998). As well as being a transcriptional target for p53, MDM2 can interfere with the transcriptional activity of p53 by direct binding via its N-terminal region (Chen *et al*., 1993; Oliner *et al*., 1993) and can target p53 for rapid destruction by ubiquitin-mediated proteolysis (Haupt *et al*., 1997; Kubbutat *et al*., 1997). Although the domains on MDM2 that bind $p14^{ARF}$ have not been defined unambiguously (data not shown and Pomerantz *et al*., 1998; Zhang *et al*., 1998), they are likely to be distinct from the p53-binding site since it is possible to form ternary complexes containing $p14^{ARF}$, MDM2 and p53 (Figure 5C). Indeed, co-precipitation of p53 and $p14^{ARF}$ was dependent on MDM2, whereas the latter two proteins can associate in the absence of p53.

Functionally, the binding of $p14^{ARF}$ to MDM2 results in the stabilization of both p53 and MDM2 (Figure 6). These effects were apparent with mouse and human MDM2 and in different cell types. Significantly, there was also an increase in the steady-state levels of MDM2 in cells co-transfected with $p14^{ARF}$ whether or not the cells expressed exogenous p53. Moreover, truncated forms of MDM2 that are impaired in their ability to invoke degradation of p53 (M.Kubbutat and K.H.Vousden, in preparation) were clearly stabilized by the co-expression of $p14^{ARF}$ (Figure 6C). While our data broadly agree with recent reports as regards the stabilization of p53 by $p14^{ARF}$ (Pomerantz *et al*., 1998; Zhang *et al*., 1998), they are the first to demonstrate stabilization of MDM2 and are clearly at odds with the findings of Zhang *et al*. (1998). These authors proposed the destabilization of MDM2 by $p14^{ARF}$ as a mechanism for releasing free p53. However, the marked accumulation of endogenous MDM2 in NARF cells expressing inducible $p14^{ARF}$, the accumulation of exogenous MDM2 in the co-transfection assays and the detection of ternary $p14^{ARF}$–p53–MDM2 complexes seem incompatible with this interpretation. In seeking an explanation for these discrepancies, we considered the possibility that different results might prevail in cell lines expressing viral oncoproteins that interfere with p53 function (Zhang *et al*., 1998). In our hands, the co-expression of HPV16 E6 did not affect the ability of $p14^{ARF}$ to stabilize MDM2 (Figure 6D).

Because of these functional links between $p14^{ARF}$ and p53, the cell cycle arrest elicited by $p14^{ARF}$ is dependent on the status of p53 (Figure 7; Kamijo *et al*., 1997; Pomerantz *et al*., 1998), in striking contrast to the pRb-dependent G_1-phase arrest imposed by $p16^{INK4a}$ (Guan *et al*., 1994; Okamoto *et al*., 1994; Koh *et al*., 1995; Lukas *et al*., 1995; Medema *et al*., 1995; Stone *et al*., 1995a). It is also clear that the effects of $p14^{ARF}$ can be negated by the presence of HPV E6 protein, which targets p53 for degradation. However, there is another important facet to the regulatory connections between p53 and $p14^{ARF}$. As demonstrated in Figure 9, the expression of $p14^{ARF}$ appears to be negatively controlled by p53, invoking intriguing parallels with the feedback loop through

which pRb influences the expression of the *CDKN2A* α transcript in human cells (Li *et al*., 1994b; Hara *et al*., 1996; Palmero *et al*., 1997). We have reported previously that in human diploid fibroblasts the transcription of exon 1β is inversely related to the function of SV40 T-antigen, although we did not draw a distinction between the effects of T-Ag on pRb or p53 in this earlier work (Hara *et al*., 1996). We now show that introduction of the HPV16 E6 protein into these cells dramatically increases the expression of $p14^{ARF}$ (Figure 9A). Moreover, direct modulation of p53 activity, using a tetracycline-regulatable expression system or with a temperature-sensitive mutant of p53, was clearly able to down-regulate the expression of endogenous $p14^{ARF}$ in SAOS2 cells (Figure 9B and C). There are as yet no definitive data to indicate whether mouse $p19^{ARF}$ expression can be modulated directly by p53 (Quelle *et al*., 1995b, 1997; Kamijo *et al*., 1997).

In our survey of human tumour cell lines, there was complete concordance between the expression of the protein and the detection of the β transcript, although a recent report showed that some haemopoietic cells express the RNA but not the protein (Della Valle *et al*., 1997). Moreover, a consistent staining pattern has been observed in different human cell lines that is similar to the nuclear speckles and nucleolar staining previously reported for mouse $p19^{ARF}$ (Figure 2; Quelle *et al*., 1995b; Della Valle *et al*., 1997). Although provocative, the significance of this staining pattern has not been explored fully. One possibility is that ARF is a component of nuclear structures that are important for some facet of DNA/RNA synthesis or processing such that excessive levels interfere with the proper function of these structures and trigger a p53-dependent growth arrest. However, it is clear that ARF plays no part in the p53-mediated response to DNA damage. Actinomycin D treatment (Figure 10) stabilizes p53 without detectable increases in $p14^{ARF}$ expression, and ARF-negative cell lines, such as A375, and the MEFs from ARF nullizygous mice (Kamijo *et al*., 1997) both show normal DNA damage-induced p53 responses. Curiously, low levels of actinomycin D caused an appreciable down-regulation of $p14^{ARF}$ in cells lacking p53. Whether this reflects the effect of actinomycin D on transcription of exon 1β or p53-independent effects on $p14^{ARF}$ stability is currently under investigation.

Taken together, our data imply that $p14^{ARF}$ is both regulated by and can regulate p53, adding a new dimension to the known feedback loops between p53 and MDM2 (Figure 11). The burning question, therefore, is what activates ARF expression? Unfortunately, the low levels of RNA and protein in primary cells have so far precluded drawing any connection with population doublings, but senescence remains an attractive possibility. For example, up-regulation of ARF as cells approach their finite lifespan could in part explain the accumulation of $p21^{CIP1}$, although the currently available data suggest that $p21^{CIP1}$ may be under p53-independent as well as p53-dependent regulation in this setting (Tahara *et al*., 1995). A strong argument in favour of this idea has come from the recent report on mice that have a targeted disruption of *CDKN2A* exon 1β (Kamijo *et al*., 1997). The mice develop normally but have a high incidence of spontaneous tumours, and the derived embryo fibroblasts do not undergo the growth arrest indicative of the M_1 phase of replicative senescence.

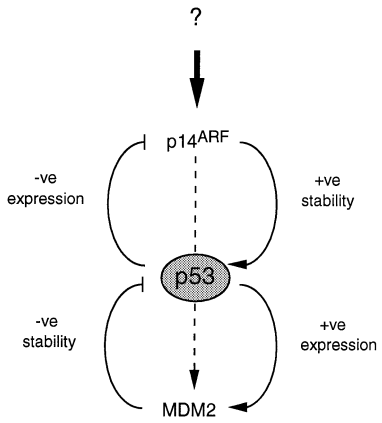

Fig. 11. A model for the regulatory loops involving $p14^{ARF}$, p53 and MDM2. Positive and negative effects are as indicated.

Since these properties resemble the phenotypes reported for mice with a targeted disruption of the shared *CDKN2A* exon 2 sequences (Serrano *et al*., 1996), it has been argued that the phenotype of the latter mice may be entirely attributable to the loss of ARF function, implicating ARF in both senescence and tumour suppression (Kamijo *et al*., 1997).

Although the data we present here are consistent with such a role for ARF, we propose a different interpretation in which parallels can be drawn between loss of ARF and loss of p53 function, rather than between ARF and $p16^{INK4a}$. In the first place, p53–/– mice sustain spontaneous tumours that are broadly similar in pathology and incidence to those reported for the *CDKN2A* exon 1β and exon 2 knockouts (Donehower *et al*., 1992; Serrano *et al*., 1996; Kamijo *et al*., 1997). In all three cases, the nullizygous embryo fibroblasts immortalize spontaneously and are sensitive to transformation by *RAS* (Harvey *et al*., 1993; Tsukuda *et al*., 1993; Serrano *et al*., 1996; Kamijo *et al*., 1997). Secondly, Kamijo *et al*. noted mutually exclusive loss of ARF or p53 during immortalization of mouse fibroblasts (Kamijo *et al*., 1997) which would be consistent with genes that function within a common pathway. A key point in their argument was that immortalization occurred without any deleterious effects on the expression or function of the $p16^{INK4a}$ protein. However, it is well known that rodent cells undergo spontaneous immortalization at an unusually high frequency compared with cells from other higher eukaryotic species, and there is a large body of evidence to indicate that dysregulation of either p53- or pRb-dependent mechanisms is sufficient to bypass senescence in cultured rodent cells (Shay *et al*., 1991b). Thus, the majority of established mouse cell lines have been shown to be defective for p53 function, whereas deletions affecting the mouse *CDKN2A* locus are comparatively rare (Harvey and Levine, 1991; Rittling and Denhardt, 1992; Linardopoulos *et al*., 1995).

In contrast, lifespan extension of human cells generally involves abrogation of both p53- and pRb-dependent pathways (Shay and Wright, 1989; Shay *et al*., 1991a), and p53 and $p16^{INK4a}$ feature prominently among the most frequently altered genes in human cancers. It has been estimated that up to 75% of established human tumour cell lines have sustained alterations that incapacitate $p16^{INK4a}$ (Ruas and Peters, 1998), confirming the strong selection

against this gene as cells escape senescence. Indeed, even cells derived from Li–Fraumeni patients, which are p53 defective, have been shown to sustain $p16^{INK4a}$ deletions during escape from senescence (Rogan *et al*., 1995; Noble *et al*., 1996). Although many of the deletions that affect $p16^{INK4a}$ also encompass $p14^{ARF}$, only a minority of the tumour-associated mutations in *CDKN2A* affect the sequence of $p14^{ARF}$ (in exon 2), and no mutations have yet been recorded in exon 1β (Ruas and Peters, 1998). Moreover, mutagenesis of exon 2 has been shown to have no effect on the known properties of ARF, and the protein encoded by exon 1β alone is sufficient to induce a cell cycle arrest (Figure 7E; Arap *et al*., 1997; Quelle *et al*., 1997). These data argue strongly against the notion that targeted disruption of exon 2 produces the same phenotype as the disruption of exon 1β.

Our data suggest an inverse correlation between p53 and $p14^{ARF}$ such that ARF is essentially below the current levels of detection in p53-positive cells. Coupled with the idea that ARF and p53 are functionally linked, we would argue that all human tumour cell lines that retain and express ARF are *de facto* p53 negative (see Table I). However, not all p53-negative cells express ARF because many of them have sustained 9p21 deletions that target $p16^{INK4a}$ and coincidentally remove exon 1β. The pattern is likely to depend on the order of events. If the deletion of 9p21 is an early event, and ARF is co-deleted, then the tumour cell line can remain wild-type for p53. Conversely, if mutation of p53 is an early event, then there would be little selection against ARF. However, the strong selection against $p16^{INK4a}$ would frequently result in co-deletion of ARF.

It is interesting to speculate about the evolutionary pressure for locating exon 1β next to $p16^{INK4a}$ and the likelihood that this occurred after the duplication that presumably gave rise to the tandem arrangement of *INK4a* and *INK4b*. One possibility is that it was driven by the fact that both genes are involved in facets of senescence. Although the current data suggest that the genes are not regulated coordinately by the p53 and pRb pathways, there may well be a common mechanism that relates their expression to population doublings or other signals. This is clearly an interesting concept that requires further investigation. Conversely, the close proximity of the two genes would also make them vulnerable to co-deletion, a curious state of affairs if both are involved in the mechanims underlying tumour suppression.

Materials and methods

Mammalian cell culture

The human tumour cell lines MCF7, BT549, MDA MB468, MDA MB231, A375, T24, 5637, U2OS, SAOS2, HaCaT, C33A, NCI H596 and H1299 were maintained at 37°C in Dulbecco's modified Eagle's medium (DMEM) supplemented with 10% fetal calf serum (FCS). The primary diploid fibroblast strains, WI38 and TIG3, and their SV40-transformed derivatives, VA13 and SVts8, respectively, were grown under the same conditions except that the SVts8 cells were kept routinely at 34°C which is permissive for the function of the temperature-sensitive form of SV40 T-Ag. The CEM and Kit225 lymphocyte cell lines were maintained in RPMI medium + 10% FCS. Kit225 cultures were supplemented with 20 ng/ml of IL-2 (from EuroCetus).

Construction of expression vectors

A cDNA encoding $p14^{ARF}$ was isolated by RT–PCR using mRNA extracted from TIG3 cells. Following first strand cDNA synthesis (Boehringer Mannheim kit), the relevant sequences were amplified by PCR using the forward and reverse primers: 5′-AGGCGGCGGATCCATGGTGCGCAGGTT-3′ and 5′-CCGAATTCTCAGCCAGGCCACG-3′. The PCR product was digested with *Bam*HI and *Eco*RI and subcloned into the corresponding sites in the Bluescript KS+ and pcDNA3 vectors. The IPTG-regulatable constructs in the pOPRSVI vector (LAC SWITCH™ from Stratagene) were engineered in a two-step process. The DNA fragments encoding $p14^{ARF}$ and $p16^{INK4a}$ were excised from the pcDNA3-based plasmids using *Xba*I and *Bam*HI and subcloned into Bluescript to exploit the *Not*I sites in the polylinker. The inserts were then recovered by digestion with *Not*I and subcloned into the *Not*I site in pOPRSVICAT. The orientation of the inserts was determined by DNA sequencing using the primers described above for PCR. Recombinant retroviruses were constructed by transferring the relevant *Bam*HI–*Eco*RI fragments into the pBABE-puro and pBABE-hygro vectors (Morgenstern and Land, 1990). The expression constructs for p53, mouse Mdm2 and human MDM2 have been described previously (Marston *et al*., 1994; Chen *et al*., 1995; Elenbaas *et al*., 1996; Kubbutat *et al*., 1997).

Transient and stable transfections

For transient transfection assays, cells were plated at a density of 2×10^5 cells per 10 cm dish. Twenty μg of pcDNA3-based plasmids were co-transfected with 7 μg of plasmid encoding the CD20 cell surface marker, using Lipofectamine (Gibco-BRL). For co-transfections with HPV E6, the amount of $p14^{ARF}$-encoding plasmid was reduced to either 5 or 10 μg to allow addition of 10 μg of the pcB6+Q369 HPV16 E6 construct. The transiently transfected cells were stained with fluorescein isothiocyanate (FITC)-conjugated anti-CD20 antibody (Becton Dickinson) to detect surface expression of CD20 and with propidium iodide to determine their relative DNA content. The proportion of CD20-positive cells in different phases of the cell cycle was then determined by fluorescence-activated cell sorting (FACS; van den Heuvel and Harlow, 1993).

IPTG-inducible expression was established in the U2OS human osteosarcoma cells using the LAC SWITCH™ vector system (Stratagene). The $p16^{INK4a}$ and $p14^{ARF}$ cDNAs in the pOPRSVI-Lac operator vector were co-transfected with the p3′SS plasmid containing the Lac repressor in a 1:1 ratio. Stable transfectants were selected with 150 μg/ml hygromycin (Sigma) and 300 μg/ml geneticin (Gibco-BRL), and after 48 h the cells were replated at a low density to allow the isolation of single colonies. The clonal cell lines derived from the transfectants, EH1 and 2 and NARF1–6, were maintained in DMEM + 10% FCS containing 150 μg/ml hygromycin and 300 μg/ml geneticin. To ensure that the cells were not metabolically challenged during various assays, the antibiotics were removed from the medium 24 h prior to assay.

Immunofluoresence

Between 5×10^4 and 1×10^5 cells seeded on coverslips in a 24-well plate were fixed in 50% methanol/50% acetone for 5 min, and blocked in 10% bovine serum albumin (BSA) for 15 min. The anti-human $p14^{ARF}$ antibody (IP1) was affinity purified against the peptide antigen using the Sulfolink coupling kit (Pierce) to immobilize the antigen. Affinity-purified serum (IP1) was incubated undiluted with the fixed cells for 45 min. The coverslips were washed twice for 3 min in phosphate-buffered saline (PBS) and incubated for 45 min with TRITC (Texas Red)-conjugated anti-rabbit secondary antibody (DAKO) diluted 1:20 in PBS. Cells were again washed twice for 3 min in PBS before mounting onto slides.

Protein analysis

Cell lysates for immunoblotting were prepared by scraping cells into 1× Laemmli buffer lacking bromophenol blue and mercaptoethanol. These lysates were boiled and the protein concentration was determined using the BCA protein assay reagent (Pierce). Balanced amounts of cell proteins (20–40 μg) were then boiled again after addition of mercaptoethanol and bromophenol blue and fractionated by SDS–PAGE in 15% acrylamide gels. After transferring the proteins onto Immobilon-P (Millipore), the membranes were blocked in 5% milk powder, 0.2% Tween-20 in PBS for 30 min and incubated with the primary antibody for 1 h. Membranes were then washed in 0.2% Tween-20 in PBS once for 15 min and three times for 5 min at room temperature. Depending on the experiment, sheep anti-mouse horseradish peroxidase (HRP) (1:1000 dilution) and donkey anti-rabbit HRP (1:2000 dilution) were used as secondary antibodies (Amersham). Antibody binding was visualized using Amersham ECL reagents. The primary antibodies used in these studies were against human $p16^{INK4a}$ (DCS50; Lukas *et al*.,

1995), human $p14^{ARF}$(IP1, this study), CDK2 (Santa Cruz M2), pRb (Pharmingen G3-245), MDM2 (Pharmingen SMP14), $p21^{CIP1}$ (Pharmingen 6B6), $p27^{KIP1}$ (Pharmingen G173-S24), p53 (DO1 and 1801), cyclin D1 (287–3; Bates *et al*., 1994a) and cyclin E (Santa Cruz C19).

For immunoprecipitation, lysates were prepared in NP-40 lysis buffer as previously described (Bates *et al*., 1994a). Protein concentrations were determined using the BCA reagents as above. For a single immunoprecipitation, 1 ml of lysate containing ~1 mg of protein was mixed with 20 µl of protein A beads and antibody, for 2 h. Precipitated proteins were separated by SDS–PAGE in 12% acrylamide gels and immunoblotted as above.

In vitro binding assay

The sequences encoding cyclin D1, Flag-tagged $p14^{ARF}$, human MDM2 and the Δ222–437 mutant were cloned into the pcDNA3 vector and expressed by coupled transcription and translation in the Promega TnT system. Selected proteins were labelled with [^{35}S]methionine and *in vitro* binding assays were performed as described previously (Parry *et al*., 1995).

p53 stability assay

MDM2-mediated degradation of p53 was analysed in transiently transfected cells as previously described (Kubbutat *et al*., 1997). Briefly, U2OS or SAOS2 cells were transfected using calcium phosphate co-precipitation with 3 µg of pCB6+p53 or pCB6+p53DI, 0–9 µg of pCOCmdm2 or pCHDM, and 0–15 µg of pcDNA3ARF (Kubbutat *et al*., 1997). Cells were harvested 24 h post-transfection and p53 expression analysed by Western blotting with the monoclonal antibody PAb1801. Equal transfection efficiency was confirmed by co-transfection of 1 µg of pEGFP-N1, and equal expression of green fluorescent protein (GFP) confirmed by Western blotting with a monoclonal antibody (Clontech). In some experiments, the LLnL proteasome inhibitor (Boehringer) was added to the culture medium at a final concentration of 50 µM.

Retroviral infection of primary fibroblasts

The TIG3 strain of human diploid fibroblasts were infected at 40–45 population doublings with an amphotropic virus encoding the mouse cationic amino acid transporter (Serrano *et al*., 1997; McConnell *et al*., 1998) and selected in G418. Cell pools subsequently were infected with recombinant ecotropic viruses based on the pBABE-puro and pBABE-hygro vectors (Morgenstern and Land, 1990) that had been packaged by transient transfection of BOSC-23 cells (Pear *et al*., 1993). Pools of cells were selected for 7 days in 50 µg/ml hygromycin and/or 0.5 µg/ml puromycin. Where appropriate, vector-only controls were set up using both pBABE-puro and pBABE-hygro with dual selection. Cell proliferation and SA-β-gal assays were performed as previously described (Dimri *et al*., 1995; Serrano *et al*., 1997; McConnell *et al*., 1998).

Acknowledgements

We are grateful to Hartmut Land, David Mann, Mike Fried and Alison Sinclair for comments on the manuscript and to Andy Phillips and Michael Kubbutat for helpful discussion and provision of reagents. The MDM2 mutants were generously provided by Arnold Levine. We also thank Robert Ludwig for additional technical help. S.B. and K.H.V. were supported by the National Cancer Institute, DHHS, under contract with ABL, and part of this work was supported by a grant from the Human Frontiers Science Program to G.P. and K.H.V.

References

Agarwal,M.L., Agarwal,A., Taylor,W.R. and Stark,G.R. (1995) p53 controls both the G2/M and the G1 cell cycle checkpoints and mediates reversible growth arrest in human fibroblasts. *Proc. Natl Acad. Sci. USA*, **92**, 8493–8497.

Alcorta,D.A., Xiong,Y., Phelps,D., Hannon,G., Beach,D. and Barrett,J.C. (1996) Involvement of the cyclin-dependent kinase inhibitor p16 (INK4a) in replicative senescence. *Proc. Natl Acad. Sci. USA*, **93**, 13742–13747.

Arap,W., Knudsen,E., Sewell,D.A., Sidransky,D., Wang,J.Y.J., Huang,H.-J.S. and Cavanee,W.K. (1997) Functional analysis of wild-type and malignant glioma derived *CDKN2A*β alleles: evidence for an RB-independent growth suppressive pathway. *Oncogene*, **15**, 2013–2020.

Barak,Y., Juven,T., Haffner,R. and Oren,M. (1993) mdm2 expression is induced by wild type p53 activity. *EMBO J.*, **12**, 461–468.

Bates,S. and Vousden,K.H. (1996) p53 in signaling checkpoint arrest or apoptosis. *Curr. Opin. Genet. Dev.*, **6**, 12–18.

Bates,S., Bonetta,L., MacAllan,D., Parry,D., Holder,A., Dickson,C. and Peters,G. (1994a) CDK6 (PLSTIRE) and CDK4 (PSK-J3) are a distinct subset of the cyclin-dependent kinases that associate with cyclin D1. *Oncogene*, **9**, 71–79.

Bates,S., Parry,D., Bonetta,L., Vousden,K., Dickson,C. and Peters,G. (1994b) Absence of cyclin D/cdk complexes in cells lacking functional retinoblastoma protein. *Oncogene*, **9**, 1633–1640.

Bates,S., Ryan,K.M., Phillips,A.C. and Vousden,K.H. (1998) Cell cycle arrest and DNA endoreduplication following $p21^{WAF1/CIP1}$ expression. *Oncogene*, in press.

Brown,J.P., Wei,W. and Sedivy,J.M. (1997) Bypass of senescence after disruption of $p21^{CIP1/WAF1}$ gene in normal diploid human fibroblasts. *Science*, **277**, 831–834.

Brugarolas,J., Chandrasekaran,C., Gordon,J.I., Beach,D., Jacks,T. and Hannon,G.J. (1995) Radiation-induced cell cycle arrest compromised by p21 deficiency. *Nature*, **377**, 552–557.

Cairns,P. *et al*. (1994) Rates of *p16* (*MTS1*) mutations in primary tumors with 9p loss. *Science*, **265**, 415–416.

Cayrol,C., Knibiehler,M. and Ducommun,B. (1998) p21 binding to PCNA causes G1 and G2 cell cycle arrest in p53-deficient cells. *Oncogene*, **16**, 311–320.

Chen,J., Marechal,V. and Levine,A.J. (1993) Mapping of the p53 and mdm-2 interaction domains. *Mol. Cell. Biol.*, **13**, 4107–4114.

Chen,J., Lin,J. and Levine,A.J. (1995) Regulation of transcription functions of the p53 tumor suppressor by the *mdm-2* oncogene. *Mol. Med.*, **1**, 142–152.

Cross,S.M., Sanchez,C.A., Morgan,C.A., Schimke,M.K., Ramel,S., Idzerda,R.L., Raskind,W.H. and Reid,B.J. (1995) A p53-dependent mouse spindle checkpoint. *Science*, **267**, 1353–1356.

Della Valle,V., Duro,D., Bernard,O. and Larsen,C.-J. (1997) The human protein $p19^{ARF}$ is not detected in hemopoietic human cell lines that abundantly express the alternative β transcript of the $p16^{INK4a}$/MTS1 gene. *Oncogene*, **15**, 2475–2481.

Deng,C., Zhang,P., Harper,J.W., Elledge,S.J. and Leder,P. (1995) Mice lacking normal $p21^{CIP1/WAF1}$ undergo normal development, but are defective in G1 checkpoint control. *Cell*, **82**, 675–684.

Diller,L. *et al*. (1990) p53 functions as a cell cycle control point in osteosarcoma. *Mol. Cell. Biol.*, **10**, 5772–5781.

Dimri,G.P. *et al*. (1995) A novel biomarker identifies senescent human cells in culture and in aging skin *in vivo*. *Proc. Natl Acad. Sci. USA*, **92**, 9363–9367.

Donehower,L.A., Harvey,M., Slagle,B.L., McArthur,M.J., Montgomery,C.A.J., Butel,J.S. and Bradley,A. (1992) Mice deficient for p53 are developmentally normal but susceptible to spontaneous tumours. *Nature*, **356**, 215–221.

Duro,D., Bernard,O., Della Valle,V., Berger,R. and Larsen,C.-J. (1995) A new type of $p16^{INK4}$/MTS1 gene transcript expressed in B-cell malignancies. *Oncogene*, **11**, 21–29.

El-Deiry,W.S. *et al*. (1993) *WAF1*, a potential mediator of p53 tumor suppression. *Cell*, **75**, 817–825.

Elenbaas,B., Dobbelstein,M., Roth,J., Shenk,T. and Levine,A.J. (1996) The MDM2 oncoprotein binds specifically to RNA through its RING finger domain. *Mol. Med.*, **2**, 439–451.

Fukasawa,K., Choi,T., Kuriyama,R., Rulong,S. and Vande Woude,G.F. (1996) Abnormal centrosome amplification in the absence of p53. *Science*, **271**, 1744–1747.

Guan,K.-L., Jenkins,C.W., Li,Y., Nichols,M.A., Wu,X., O'Keefe,C.L., Matera,A.G. and Xiong,Y. (1994) Growth suppression by *p18*, a $p16^{INK4/MTS1}$ and $p14^{INK4/MTS2}$-related CDK6 inhibitor, correlates with wild-type pRb function. *Genes Dev.*, **8**, 2939–2952.

Hainaut,P., Soussi,T., Shomer,B., Hollstein,M., Greenblatt,M., Hovig,E., Harris,C.C. and Montesano,R. (1997) Database of p53 gene somatic mutations in human tumors and cell lines: updated compilation and future prospects. *Nucleic Acids Res.*, **25**, 151–157.

Hara,E., Tsurui,H., Shinozaki,A., Nakada,S. and Oda,K. (1991) Cooperative effect of antisense-Rb and antisense-p53 oligomers on the extension of life span of human diploid fibroblasts, TIG-1. *Biochem. Biophys. Res. Commun.*, **179**, 528–534.

Hara,E., Smith,R., Parry,D., Tahara,H., Stone,S. and Peters,G. (1996) Regulation of $p16^{CDKN2}$ expression and its implications for cell immortalization and senescence. *Mol. Cell. Biol.*, **16**, 859–867.

Harper,J.W. *et al*. (1995) Inhibition of cyclin-dependent kinases by p21. *Mol. Biol. Cell*, **6**, 387–400.

Harvey,D.M. and Levine,A.J. (1991) p53 alteration is a common event in the spontaneous immortalization of primary BALB/c murine embryo fibroblasts. *Genes Dev.*, **5**, 2375–2385.

Harvey,M. *et al*. (1993) *In vitro* growth characteristics of embryo fibroblasts isolated from p53-deficient mice. *Oncogene*, **8**, 2457–2467.

Haupt,Y., Maya,R., Kazaz,A. and Oren,M. (1997) Mdm2 promotes the rapid degradation of p53. *Nature*, **387**, 296–299.

Horowitz,J.M., Park,S.-H., Bogenmann,E., Cheng,J.-G., Yandell,D.W., Kaye,F.J., Minna,J.D., Dryja,T.P. and Weinberg,R.A. (1990) Frequent inactivation of the retinoblastoma anti-oncogene is restricted to a subset of human tumor cells. *Proc. Natl Acad. Sci. USA*, **87**, 2775–2779.

Jiang,P., Stone,S., Wagner,R., Wang,S., Dayananth,P., Kozak,C.A., Wold,B. and Kamb,A. (1995) Comparative analysis of *Homo sapiens* and *Mus musculus* cyclin-dependent kinase (CDK) inhibitor genes P16 (MTS1) and P15 (MTS2). *J. Mol. Evol.*, **41**, 795–802.

Kamb,A. *et al*. (1994) A cell cycle regulator potentially involved in genesis of many tumor types. *Science*, **264**, 436–440.

Kamijo,T., Zindy,F., Roussel,M.F., Quelle,D.E., Downing,J.R., Ashmun,R.A., Grosveld,G. and Sherr,C.J. (1997) Tumor suppression at the mouse *INK4a* locus mediated by the alternative reading frame product $p19^{ARF}$. *Cell*, **91**, 649–659.

Koh,J., Enders,G.H., Dynlacht,B.D. and Harlow,E. (1995) Tumour-derived p16 alleles encoding proteins defective in cell-cycle inhibition. *Nature*, **375**, 506–510.

Kubbutat,M.H.G., Jones,S.N. and Vousden,K.H. (1997) Regulation of p53 stability by Mdm2. *Nature*, **287**, 299–303.

Larsen,C.-J. (1996) $p16^{INK4a}$: a gene with a dual capacity to encode unrelated proteins that inhibit cell cycle progression. *Oncogene*, **12**, 2041–2044.

Levine,A.J. (1997) p53, the cellular gatekeeper for growth and division. *Cell*, **88**, 323–331.

Li,Y., Jenkins,C.W., Nichols,M.A. and Xiong,Y. (1994a) Cell cycle expression and p53 regulation of the cyclin-dependent kinase inhibitor p21. *Oncogene*, **9**, 2261–2268.

Li,Y., Nichols,M.A., Shay,J.W. and Xiong,Y. (1994b) Transcriptional repression of the D-type cyclin-dependent kinase inhibitor p16 by the retinoblastoma susceptibility gene product pRb. *Cancer Res.*, **54**, 6078–6082.

Liggett,W.H.J., Sewell,D.A., Rocco,J., Ahrendt,S.A., Koch,W. and Sidransky,D. (1996) *p16* and *p16*β are potent growth suppressors of head and neck squamous carcinoma cells *in vitro*. *Cancer Res.*, **56**, 4119–4123.

Linardopoulos,S., Street,A.J., Quelle,D.E., Parry,D., Peters,G., Sherr,C.J. and Balmain,A. (1995) Deletion and altered regulation of $p16^{INK4a}$ and $p15^{INK4b}$ in undifferentiated mouse skin tumors. *Cancer Res.*, **55**, 5168–5172.

Lloyd,A.C., Obermuller,F., Staddon,S., Barth,C.F., McMahon,M. and Land,H. (1997) Cooperating oncogenes converge to regulate cyclin/cdk complexes. *Genes Dev.*, **11**, 663–677.

Loughran,O., Malliri,A., Owens,D., Gallimore,P.H., Stanley,M.A., Ozanne,B., Frame,M.C. and Parkinson,E.K. (1996) Association of CDKN2A/$p16^{INK4A}$ with human head and neck keratinocyte replicative senescence: relationship of dysfunction to immortality and neoplasia. *Oncogene*, **13**, 561–568.

Lukas,J., Parry,D., Aagaard,L., Mann,D.J., Bartkova,J., Strauss,M., Peters,G. and Bartek,J. (1995) Retinoblastoma-protein-dependent cell cycle inhibition by the tumour suppressor p16. *Nature*, **375**, 503–506.

Lukas,J., Petersen,B.O., K,H., Bartek,J. and Helin,K. (1996) Deregulated expression of E2F family members induces S-phase entry and overcomes $p16^{INK4A}$-mediated growth suppression. *Mol. Cell. Biol.*, **16**, 1047–1057.

Mann,D.J. and Jones,N.C. (1996) E2F-1 but not E2F-4 can overcome p16-induced G1 cell cycle arrest. *Curr. Biol.*, **6**, 474–483.

Mao,L., Merlo,A., Bedi,G., Shapiro,G.I., Edwards,C.D., Rollins,B.J. and Sidransky,D. (1995) A novel $p16^{INK4A}$ transcript. *Cancer Res.*, **55**, 2995–2997.

Marston,N.J., Crook,T. and Vousden,K.H. (1994) Interaction of p53 with MDM2 is independent of E6 and does not mediate wild type transformation suppressor function. *Oncogene*, **9**, 2707–2716.

McConnell,B.B., Starborg,M., Brookes,S. and Peters,G. (1998) Inhibitors of cyclin-dependent kinases induce features of replicative senescence in early passage human diploid fibroblasts. *Curr. Biol.*, **8**, 351–354.

Medema,R., Herrera,R.E., Lam,F. and Weinberg,R.A. (1995) Growth suppression by $p16^{INK4}$ requires functional retinoblastoma protein. *Proc. Natl Acad. Sci. USA*, **92**, 6289–6293.

Medema,R.H., Klompmaker,R., Smits,V.A.J. and Rijksen,G. (1998) $p21^{waf1}$ can block cells at two points in the cell cycle, but does not interfere with processive DNA-replication or stress-activated kinases. *Oncogene*, **16**, 431–441.

Morgenstern,J.P. and Land,H. (1990) Advanced mammalian gene transfer: high titre retroviral vectors with multiple drug selection markers and a complementary helper-free packaging cell line. *Nucleic Acids Res.*, **18**, 3587–3596.

Niculescu,A.B.,III, Chen,X., Smeets,M., Hengst,L., Prives,C. and Reed,S.I. (1998) Effects of $p21^{Cip1/Waf1}$ at both the G_1/S and the G_2/M cell cycle transitions: pRb is a critical determinant in blocking DNA replication and in preventing endoreduplication. *Mol. Cell. Biol.*, **18**, 629–643.

Noble,J.R., Rogan,E.M., Neumann,A.A., Maclean,K., Bryan,T.M. and Reddel,R.R. (1996) Association of extended *in vitro* proliferative potential with loss of $p16^{INK4}$ expression. *Oncogene*, **13**, 1259–1268.

Nobori,T., Miura,K., Wu,D.J., Lois,A., Takabayashi,K. and Carson,D.A. (1994) Deletions of the cyclin-dependent kinase-4 inhibitor gene in multiple human cancers. *Nature*, **368**, 753–756.

Noda,A., Ning,Y., Venable,S.F., Pereira-Smith,O.M. and Smith,J.R. (1994) Cloning of senescent cell-derived inhibitors of DNA synthesis using an expression screen. *Exp. Cell Res.*, **211**, 90–98.

Okamoto,A. *et al*. (1994) Mutations and altered expression of $p16^{INK4}$ in human cancer. *Proc. Natl Acad. Sci. USA*, **91**, 11045–11049.

Oliner,J.D., Pietenpol,J.A., Thiagalingam,S., Gyuris,J., Kinzler,K.W. and Vogelstein,B. (1993) Oncoprotein MDM2 conceals the activation domain of tumour suppressor p53. *Nature*, **362**, 857–860.

Palmero,I., McConnell,B., Parry,D., Brookes,S., Hara,E., Bates,S., Jat,P. and Peters,G. (1997) Accumulation of $p16^{INK4a}$ in mouse fibroblasts as a function of replicative senescence and not of retinoblastoma gene status. *Oncogene*, **15**, 495–503.

Parry,D., Bates,S., Mann,D.J. and Peters,G. (1995) Lack of cyclin D–Cdk complexes in Rb-negative cells correlates with high levels of $p16^{INK4/MTS1}$ tumour suppressor gene product. *EMBO J.*, **14**, 503–511.

Pear,W.S., Nolan,G.P., Scott,M.L. and Baltimore,D. (1993) Production of high-titer helper-free retroviruses by transient transfection. *Proc. Natl Acad. Sci. USA*, **90**, 8392–8396.

Pomerantz,J. *et al*. (1998) The *Ink4a* tumor suppressor gene product, $p19^{Arf}$, interacts with MDM2 and neutralizes MDM2′s inhibition of p53. *Cell*, **92**, 713–723.

Quelle,D.E. *et al*. (1995a) Cloning and characterization of murine $p16^{INK4a}$ and $p15^{INK4b}$ genes. *Oncogene*, **11**, 635–645.

Quelle,D.E., Zindy,F., Ashmun,R.A. and Sherr,C.J. (1995b) Alternative reading frames of the *INK4a* tumor suppressor gene encode two unrelated proteins capable of inducing cell cycle arrest. *Cell*, **83**, 993–1000.

Quelle,D.E., Cheng,M., Ashmun,R.A. and Sherr,C.J. (1997) Cancer-associated mutations at the *INK4a* locus cancel cell cycle arrest by $p16^{INK4a}$ but not by the alternative reading frame protein $p19^{ARF}$. *Proc. Natl Acad. Sci. USA*, **94**, 669–673.

Reznikoff,C.A., Yeager,T.R., Belair,C.A., Savelieva,E., Puthenveettil,J.A. and Stadler,W.M. (1996) Elevated p16 at senescence and loss of p16 at immortalization in human papillomavirus 16 E6, but not E7, transformed human uroepithelial cells. *Cancer Res.*, **56**, 2886–2890.

Rittling,S.R. and Denhardt,D.T. (1992) p53 mutations in spontaneously immortalized 3T12 but not 3T3 mouse embryo cells. *Oncogene*, **7**, 935–943.

Rogan,E.M. *et al*. (1995) Alterations in p53 and $p16^{INK4}$ expression and telomere length during spontaneous immortalization of Li–Fraumeni syndrome fibroblasts. *Mol. Cell. Biol.*, **15**, 4745–4753.

Ruas,M. and Peters,G. (1998) The $p16^{INK4a}$ tumor suppressor and its relatives. *Biochim. Biophys. Acta*, in press.

Scheffner,M., Werness,B., Huibregtse,J.M., Levine,A.J. and Howley,P.M. (1990) The E6 oncoprotein encoded by human papilloma virus types 16 and 18 promotes the degradation of p53. *Cell*, **63**, 1129–1136.

Serrano,M., Hannon,G.J. and Beach,D. (1993) A new regulatory motif in cell-cycle control causing specific inhibition of cyclin D/CDK4. *Nature*, **366**, 704–707.

Serrano,M., Lee,H.-W., Chin,L., Cordon-Cardo,C., Beach,D. and DePinho,R.A. (1996) Role of the *INK4a* locus in tumor suppression and cell mortality. *Cell*, **85**, 27–37.

Serrano,M., Lin,A.W., McCurrach,M.E., Beach,D. and Lowe,S.W. (1997) Oncogenic *ras* provokes premature cell senescence associated with accumulation of p53 and $p16^{INK4a}$. *Cell*, **88**, 593–602.

Sewing,A., Wiseman,B., Lloyd,A.C. and Land,H. (1997) High-intensity Raf signal causes cell cycle arrest mediated by $p21^{CIP1}$. *Mol. Cell. Biol.*, **17**, 5588–5597.

Shay,J.W. and Wright,W.E. (1989) Quantitation of the frequency of immortalization of normal human diploid fibroblasts by SV40 large T-antigen. *Exp. Cell*. Res., **184**, 109–118.

Shay,J.W., Pereira-Smith,O.M. and Wright,W.E. (1991a) A role for both RB and p53 in the regulation of human cellular senescence. *Exp. Cell Res.*, **196**, 33–39.

Shay,J.W., Wright,W.E. and Werbin,H. (1991b) Defining the molecular mechanisms of human cell immortalization. *Biochim. Biophys. Acta*, **1072**, 1–7.

Sherr,C.J. (1996) Cancer cell cycles. *Science*, **274**, 1672–1677.

Sherr,C.J. and Roberts,J.M. (1995) Inhibitors of mammalian G_1 cyclin-dependent kinases. *Genes Dev.*, **9**, 1149–1163.

Sidransky,D. (1996) Two tracks but one race? *Curr. Biol.*, **6**, 523–525.

Spruck,C.H.,III, Gonzales-Zulueta,M., Shibata,A., Simoneau,A.R., Lin,M.-F., Gonzales,F., Tsai,Y.C. and Jones,P.A. (1994) p16 gene in uncultured tumours. *Nature*, **370**, 183–184.

Stewart,N., Hicks,G.G., Paraskevas,F. and Mowat,M. (1995) Evidence for a second cell cycle block at G2/M by p53. *Oncogene*, **10**, 109–115.

Stone,S., Dayanath,P., Jiang,P., Weaver-Feldhaus,J.M., Tavtigian,S.V., Cannon-Albright,L. and Kamb,A. (1995a) Genomic structure, expression and mutational analysis of the P15 (MTS2) gene. *Oncogene*, **11**, 987–991.

Stone,S., Jiang,P., Dayanath,P., Tavtigian,S.V., Katcher,H., Parry,D., Peters,G. and Kamb,A. (1995b) Complex structure and regulation of the *P16* (*MTS1*) locus. *Cancer Res.*, **55**, 2988–2994.

Swafford,D.S., Middleton,S.K., Palmisano,W.A., Nikula,K.J., Tesfaigzi,J., Baylin,S.B., Herman,J.G. and Belinsky,S.A. (1997) Frequent aberrant methylation of $p16^{INK4a}$ in primary rat lung tumors. *Mol. Cell. Biol.*, **17**, 1366–1374.

Tahara,H., Sato,E., Noda,A. and Ide,T. (1995) Increase in expression level of $p21^{sdi1/cip1/waf1}$ with increasing division age in both normal and SV40-transformed human fibroblasts. *Oncogene*, **10**, 835–840.

Tsukuda,T. *et al*. (1993) Enhanced proliferative potential in culture of cells from p53-deficient mice. *Oncogene*, **8**, 3313–3322.

van den Heuvel,S. and Harlow,E. (1993) Distinct roles for cyclin-dependent kinases in cell cycle control. *Science*, **262**, 2050–2054.

Weinberg,R.A. (1995) The retinoblastoma protein and cell cycle control. *Cell*, **81**, 323–330.

Wong,H. and Riabowol,K. (1996) Differential CDK-inhibitor gene expression in aging human diploid fibroblasts. *Exp. Gerentol*., **31**, 311–325.

Woods,D., Parry,D., Cherwinsky,H., Bosch,E., Lees,E. and McMahon,M. (1997) Raf-induced proliferation or cell cycle arrest is determined by the level of Raf activity with arrest mediated by $p21^{Cip1}$. *Mol. Cell. Biol.*, **17**, 5598–5611.

Wright,W.E., Pereira Smith,O.M. and Shay,J.W. (1989) Reversible cellular senescence: implications for immortalization of normal human diploid fibroblasts. *Mol. Cell. Biol.*, **9**, 3088–3092.

Wu,X., Bayle,J.H., Olson,D. and Levine,A.J. (1993) The p53–mdm-2 autoregulatory feedback loop. *Genes Dev.*, **7**, 1126–1132.

Zhang,Y., Xiong,Y. and Yarbrough,W.G. (1998) ARF promotes MDM2 degradation and stabilizes p53: *ARF–INK4a* locus deletion impairs both the Rb and p53 tumor suppression pathways. *Cell*, **92**, 725–734.

Zindy,F., Quelle,D.E., Roussel,M.F. and Sherr,C.J. (1997) Expression of the $p16^{INK4A}$ tumor suppressor versus other INK4 family members during mouse development and aging. *Oncogene*, **15**, 203–211.

Received May 8, 1998; revised July 2, 1998; accepted July 6, 1998